Inorg. Chem. **2004**, *43*, 6726–6733

Decomposition Kinetics of Ni(III)–Peptide Complexes with Histidine and Histamine as the Third Residue

Teweldemedhin M. Tesfai, Brandon J. Green, and Dale W. Margerum*

Department of Chemistry, Purdue University, West Lafayette, Indiana 47907-2084

Received May 21, 2004

The decomposition kinetics of the Ni(III) complexes of $Gly_2HisGly$ and Gly_2Ha are studied from p[H^+] 3.5 to 10, where His is L-histidine and Ha is histamine. In these redox reactions, at least two Ni(III) complexes are reduced to Ni(II) while oxidizing a single peptide ligand. The rate of Ni(III) loss is first order at low pH, mixed order from pH 7.0 to 8.5, and second order at higher pH. The transition from first- to second-order kinetics is attributed to the formation of an oxo-bridged Ni(III)–peptide dimer. The rates of decay of the Ni(III) complexes are general-base assisted with Brønsted β values of 0.62 and 0.59 for Ni(III)$Gly_2HisGly$ and Ni(III)Gly_2Ha, respectively. The coordination of $Gly_2HisGly$ and Gly_2Ha to Ni(II) are examined by UV–vis and CD spectroscopy. The square planar $Ni^{II}(H_{-2}Gly_2HisGly)^-$ and $Ni^{II}(H_{-2}Gly_2Ha)$ complexes lose an additional proton from an imidazole nitrogen at high pH with pK_a values of 11.74 and 11.54, respectively. The corresponding Ni(III) complexes have axially coordinated water molecules with pK_a values of 9.37 and 9.44. At higher pH an additional proton is lost from the imidazole nitrogen with a pK_a value of 10.50 to give $Ni^{III}(H_{-3}Gly_2Ha)(H_2O)(OH)^{2-}$.

Introduction

Glycylglycyl-L-histidine, when attached to various binding agents or proteins in the presence of Ni(II) salts and oxidants, can cause site-specific DNA cleavage,[1−4] protein−protein cross-linking[5,6] or protein cleavage.[7] N-terminal peptide residues can coordinate to metal ions, such as Cu(II)[8] and Ni(II),[9] through the amine nitrogen and three consecutive peptide nitrogens. Ni(II)−peptide complexes containing an imidazole group in the third residue are more stable[10] than those without an imidazole nitrogen donor.[11] In the presence of O_2, Ni(II)GlyGlyHis is oxidized to a Ni(III) complex that undergoes rapid decarboxylation to give Ni(II)GlyGly-α-OH−Ha (where Ha is histamine).[12] The crystal structure of the latter species shows a square-planar complex, chelated by the amine terminal nitrogen, two deprotonated peptide nitrogens, and a histidyl imidazole nitrogen. Nickel(II)−peptide complexes can be oxidized to a +3 oxidation state either chemically or electrochemically.[13,14] Peptide complexes of nickel(III/II) have been characterized by electron paramagnetic resonance (EPR),[14−16] electrochemistry,[11,13] UV−vis,[12,17] and circular dichroism.[18−20] EPR studies have shown that Ni(III)−peptide complexes have tetragonally elongated geometry with water molecules in the axial sites.

We have recently investigated the self-decomposition products of $Ni^{III}(H_{-2}Gly_2HisGly)$.[10] In the present study, the

* To whom correspondence should be addressed. E-mail: margerum@purdue.edu.

(1) Mack, D. P.; Dervan, P. B. *J. Am. Chem. Soc*. **1990**, *112*, 4604−4606.
(2) Mack, D. P.; Dervan, P. B. *Biochemistry* **1990**, *31*, 9399−9405.
(3) Nagaoka, M.; Hagihara, M.; Kuwahara, J.; Sugiura, Y. *J. Am. Chem. Soc*. **1994**, *116*, 4085−4086.
(4) Liang, Q.; Ananias, D. C.; Long, E. C. *J. Am. Chem. Soc*. **1998**, *120*, 248−257.
(5) Brown, K.; Yang, S. H.; Kodadek, T. *Biochemistry* **1995**, *34*, 4733−4739.
(6) Brown, K. C.; Yu, Z.; Burlingame, A. L.; Craik, C. S. *Biochemistry* **1998**, *37*, 4797−4406.
(7) Cuenoud, B.; Tarasow, T. M.; Schepartz, A. *Tetrahedron Lett*. **1992**, *33*, 895−898.
(8) Peters, T., Jr.; Blumenstock, F. A. *J. Biol. Chem.* **1967**, *242*, 1574−1578.
(9) Freeman, H. C.; Guss, J. M.; Sinclair, R. L. *Chem. Commun*. **1968**, 485−487.
(10) Green, B. J,; Tesfai, T. M.; Xie, Y.; Margerum, D. W. *Inorg. Chem.* **2004**, *43*, 1463−1471.
(11) Kennedy, W. R.; Margerum, D. W. *Inorg. Chem.* **1985**, *24*, 2490−2495.
(12) Bal, W.; Djuran, M. I.; Margerum, D. W.; Gray, E. T., Jr.; Mazid, M. A.; Tom, R. T.; Nieboer, E.; Sadler, P. J. *J. Chem. Soc., Chem. Commun.* **1994**, 1889−1890.
(13) Bossu, F. P.; Margerum, D. W. *J. Am. Chem. Soc*. **1976**, *98*, 4003−4004.
(14) Bossu, F. P.; Margerum, D. W. *Inorg. Chem.* **1977**, *16*, 1210−1214.
(15) Lappin, A. G.; Murray, C. K.; Margerum, D. W. *Inorg. Chem*. **1978**, *17*, 1630−1634.
(16) Sugiura, Y.; Mino, Y. *Inorg. Chem*. **1979**, *18*, 1336−1339.
(17) Youngblood, M. P.; Margerum, D. W. *Inorg. Chem*. **1980**, *19*, 3068−3072.
(18) Czarnecki, J. J.; Margerum, D. W. *Inorg. Chem*. **1977**, *16*, 1997−2003.
(19) Chang, J. W.; Martin, R. B. *J. Phys. Chem*. **1969**, *73*, 4277−4283.
(20) Bal, W.; Jezowska-Bojczuk, M.; Kasprzak, K. S. *Chem. Res. Toxicol*. **1997**, *10*, 906−914.

10.1021/ic049338a CCC: $27.50
Published on Web 08/31/2004

reaction kinetics of Ni(III) complexes of $Gly_2HisGly$ and Gly_2Ha are examined over a wide pH range. Below pH 7.0 the redox stoichiometry is given in eq 1, where P is Gly_2-HisGly or Gly_2Ha and P_{ox} is oxidized peptide product. For these reactions, $n = 4$ for the $Gly_2HisGly$ complex and $n = 2$ for the Gly_2Ha species. Above pH 8.5 a cross-linked

$$n\mathrm{Ni^{III}(H_{-2}P)(H_2O)_2} + n\mathrm{OH^-} \rightarrow \mathrm{Ni^{II}(H_{-2}P_{ox})} + (n-1)\mathrm{Ni^{II}(H_{-2}P)} + 2n\mathrm{H_2O} \quad (1)$$

peptide (P−P) is formed, and the redox stoichiometry is given in eq 2. Imidazole deprotonation constants

$$2\mathrm{Ni^{III}(H_{-2}P)(H_2O)_2} \rightarrow (\mathrm{Ni^{II}H_{-2}})_2\text{(P-P)} + 4\mathrm{H_2O} \quad (2)$$

of Ni(II) complexes of $Gly_2HisGly$ and Gly_2Ha above p[H^+] 11 are also evaluated by UV spectral measurements. In addition, imidazole and axial water deprotonation constants of the corresponding Ni(III) complexes are measured spectroscopically and electrochemically.

Experimental Section

Reagents. Gly_2-L-HisGly and Gly_4 were obtained from BACHEM Biosciences, Inc. Gly_2Ha and Gly_2-L-AlaGly were synthesized by Dr. H. D. Lee at the Purdue University Micoanalytical Lab. All solutions were prepared with doubly deionized, distilled water. Stock solutions of carbonate-free NaOH were prepared and standardized with potassium hydrogen phthalate. A stock solution of $Ni(ClO_4)_2$ was prepared and standardized by titration with EDTA with Murexide as the indicator. EDTA was standardized titrimetrically with NaOH using Erichrome Black T as the indicator.

Methods. Nickel(II)−peptide complexes were prepared by dissolving 5−10% excess peptide in water, adding $Ni(ClO_4)_2$, and adjusting the pH to > 7. Ni(III)$Gly_2HisGly$ and Ni(III)Gly_2Ha complexes were generated electrochemically at 0.82 V (vs Ag/AgCl) by passing the corresponding Ni(II)−peptide solution at a flow rate of 0.9 mL/min through a graphite powder working electrode that was packed in a Vycor porous-glass column and wrapped with a platinum-wire auxiliary electrode.[21] An Orion Model SA 720A Research pH meter equipped with a Corning combination electrode was used to measure pH values that were corrected to p[H^+] values at $\mu = 1.0$ M ($NaClO_4$), where p[H^+] = −log([H^+]). UV−vis spectra were obtained with a Perkin-Elmer Lambda-9 UV−vis−near-IR spectrophotometer. An Applied PhotoPhysics model SX-18MV stopped-flow spectrometer (optical path length = 0.962 cm) was used to study the rate of decay of Ni(III)−peptide complexes. A PD.1 Photodiode Array (Applied PhotoPhysics) with a deuterium light source was used to obtain spectra at high pH where the rate of Ni(III) decay was rapid. Circular dichroism (CD) spectra were obtained with a Jasco Model J810 CD spectropolarimeter with a 1 cm quartz cell. All physical measurements were taken at 25.0 (±0.1) °C.

Reduction potentials were determined by Osteryoung square-wave voltammetry (OSWV) with a BAS-100 electrochemical analyzer. The working electrode was a planar glassy carbon electrode (3 mm diameter), the auxiliary electrode was platinum wire, and the reference electrode was a Vycor tip Ag/AgCl electrode stored in 3 M NaCl ($E° = 0.194$ V vs NHE).

(21) Raycheba, J. M.; Margerum, D. W. *Inorg. Chem.* **1981**, *20*, 1441−1446.

Table 1. Molar Absorptivities, Ellipticities, and Deprotonation Constants of Ni(II)−Peptide Complexes at 25.0 °C and $\mu = 1.0$ M

species	ϵ, $M^{-1}\,cm^{-1}$ (λ, nm)	$\Delta\epsilon$, $M^{-1}\,cm^{-1}$ (λ, nm)	pK_a
$Ni^{II}(H_{-2}Gly_2HisGly)^-$	11 (307)	2.57 (412)	11.74(2)
	129 (424)	−0.85 (483)	
$Ni^{II}(H_{-3}Gly_2HisGly)^{2-}$	65 (307)	3.29 (412)	
	141 (424)	−1.55 (483)	
$Ni^{II}(H_{-3}Gly_2AlaGly)^{2-}$		−1.3 (457)	
$Ni^{II}(H_{-2}Gly_2Ha)$	9 (307)		11.54(3)
	138 (424)		
$Ni^{II}(H_{-3}Gly_2Ha)^-$	63 (307)		
	138 (424)		

Results and Discussion

Spectral Characteristics of Ni(II)−Peptide Complexes. At physiological pH, the coordination of $Gly_2HisGly$[10] and Gly_2Ha[22] to Ni(II) is by the NH_2-terminus, two deprotonated peptide nitrogens, and the π nitrogen of imidazole. Gajda et al. used potentiometric and NMR data to show that deprotonation of the imidazole nitrogen occurs with a pK_a of 11.52 ($\mu = 0.1$ M) to give a $Ni^{II}(H_{-3}Gly_2Ha)^-$ species.[22] The present work shows that UV spectroscopy also can be used to measure the loss of an imidazole proton from the Ni(II)-$Gly_2HisGly$ and Ni(II)Gly_2Ha complexes. UV−vis absorbance data from p[H^+] 8.0 to 13.5 are shown in Figures 1A and S1A. Above p[H^+] 10, Ni(II) complexes of Gly_2Ha and $Gly_2HisGly$ exhibited a band growth centered at 307 nm due to the triply deprotonated complexes. The deprotonation constants of the complexes were determined by fitting the observed absorbance data at 307 nm versus p[H^+] to eq 3. The cell path, l, was 5.00 cm, and the molar absorptives (ϵ) are given in Table 1. The pK_a values obtained in Figures 1B and S1B were 11.54(3) for $Ni^{II}(H_{-2}Gly_2Ha)$, in excellent agreement with the NMR data,[22] and 11.74(2) for $Ni^{II}(H_{-2}$-$Gly_2HisGly)^-$. The increase in

$$A_{\mathrm{observed}} = [\mathrm{Ni(II)peptide}]_{\mathrm{tot}} l \left(\frac{\epsilon_{\mathrm{H-2}}[\mathrm{H^+}] + \epsilon_{\mathrm{H-3}} K_a}{K_a + [\mathrm{H^+}]} \right) \quad (3)$$

absorbance in both complexes is due to deprotonation of the imidazole ring. Other Ni(II)−peptide complexes with coordination by an N-terminal amine and three consecutive deprotonated peptide nitrogens, such as $Ni^{II}(H_{-3}Gly_4)^{2-}$, do not show absorption bands at 307 nm even in 0.1 M NaOH (Figure S10).

At p[H^+] 8.7 the $Ni^{II}(H_{-2}Gly_2$-L-HisGly$)^-$ complex, with a 5−5−six-membered ring, has a maximum ellipticity at 412 and a minimum at 483 nm in the CD spectrum (Figure 2A). These positive (412 nm) and negative (483 nm) bands increase in ellipticity as a function of p[H^+], in agreement with the changes observed in the UV−vis spectrum at 307 nm and are attributed to the deprotonation of the complex to give $Ni^{II}(H_{-3}Gly_2$-L-His$)^-$. The above CD spectrum was compared with the CD spectrum of $Ni^{II}(H_{-2}Gly_2$-L-AlaGly$)^-$.

(22) Gajda, T.; Henry, B.; Aubry, A.; Depuech, J. J. *Inorg. Chem.* **1996**, *35*, 586−593.

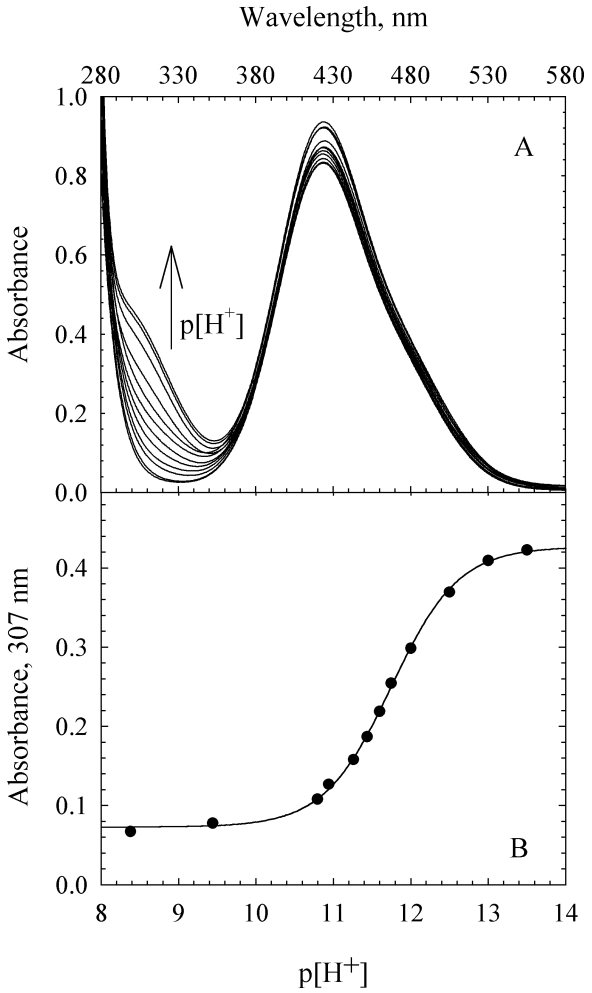

Figure 1. (A) A series of absorbance spectra for Ni(II)Gly_2HisGly. The increase in absorbance at 307 nm is observed as p[H^+] is increased from 8 to 13.5. (B) Dependence of absorbance on p[H^+] for Ni(II)Gly_2HisGly at 307 nm. The least-squares fit gives a pK_a value of 11.74(2) for the loss of an imidazole proton. Conditions: [Ni^{2+}] = 1.30 mM, [Gly_2HisGly] = 1.51 mM, μ = 1.0 M, 25.0 °C, path length = 5.00 cm.

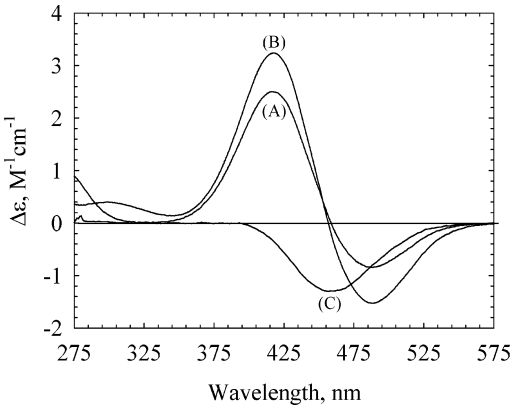

Figure 2. Circular dichroic spectra of (A) $Ni^{II}(H_{-2}Gly_2HisGly)^-$ at p[H^+] 8.7, (B) $Ni^{II}(H_{-3}Gly_2HisGly)^{2-}$ at p[H^+] 13.0, and (C) $Ni^{II}(H_{-3}Gly_2AlaGly)^{2-}$ at p[H^+] 11.5, 25.0(1) °C.

Gly_2-L-AlaGly has an asymmetric carbon on the third residue and would mimic Gly_2-L-HisGly if the latter were to coordinate Ni(II) with the terminal amine nitrogen and three consecutive deprotonated peptide nitrogens at p[H^+] higher than 12. $Ni^{II}(H_{-2}Gly_2$-L-AlaGly$)^-$ has a 5−5−five-membered

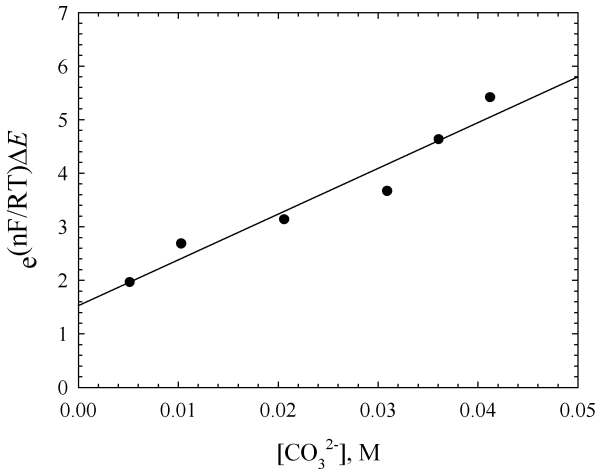

Figure 3. Electrode potential dependence on [CO_3^{2-}]. Conditions: 25.0 °C, μ = 1.0 M, p[H^+] = 8.98, [Ni(II)Gly_2Ha] = 1.0 × 10^{-3} M. Slope = K_{CO3} = 85(10) M^{-1}.

Scheme 1. Proposed Structures for $Ni^{III}(H_{-2}Peptide)(H_2O)_2^{+/0}$ and $Ni^{III}(H_{-2}Peptide)(H_2O)(CO_3)^{-/2-}$

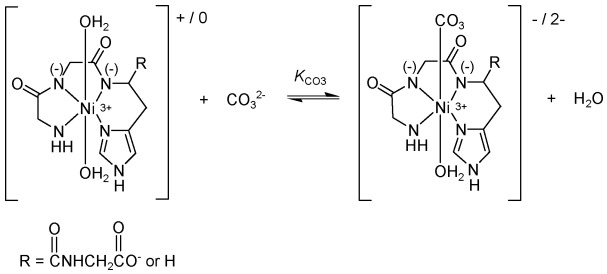

ring and gives a negative ellipticity at 457 nm that is not observed for the $Ni^{II}(H_{-2}Gly_2$-L-HisGly$)^-$ complex. Because the CD signal is dependent upon the nature of the coordinating groups,[19] the difference in CD spectra of $Ni^{II}(H_{-3}Gly_2$-L-AlaGly$)^{2-}$ and $Ni^{II}(H_{-3}Gly_2$-L-His$)^-$ indicates that the imidazole nitrogen is the observed source of the ionized proton. A similar conclusion was reached when Cu(II) complexes of the same peptides were characterized.[23]

Measurement of the Ni(III,II) Electrode Potential as a Function of Carbonate. Kinetic data obtained as a function of [CO_3^{2-}] showed that the rate of decay of the Ni(III) complexes decreases as the carbonate buffer concentration increases. Suppression of the rate of decay is attributed to the displacement of an axial water molecule by carbonate (Scheme 1). Axial coordination of carbonate appears to increase the kinetic stability of the Ni(III) complex by decreasing its reduction potential. Equilibrium constants for the coordination of carbonate to the Ni(III)Gly_2Ha and Ni(III)Gly_2HisGly complexes were determined by measuring the shift of the formal reduction potentials with the carbonate concentration. A similar method has been used to determine equilibrium constants for a variety of Ni(III)−peptide complexes with monodentate ligands.[24] At constant pH 8.98, the $E°$ change with [CO_3^{2-}] (Figure 3) is attributed to the replacement of an axial H_2O by CO_3^{2-} in the Ni(III) complex (the Ni(II) complex has no axial coordination). A decrease

(23) Tesfai, T. M.; Margerum, D. W. *Inorg. Chem.* Submitted for publication.
(24) Murray, C. K.; Margerum, D. W. *Inorg. Chem.* **1982**, *21*, 3501−3506.

in the electrode potentials was observed above p[H$^+$] 9 in low carbonate concentration. The lower potential is attributed to the deprotonation of the axially coordinated water (K_{a1}, eq 5 and Figure S9). Equations 4, 5, and 6 were used in eq 7 to evaluate the equilibrium constant K_{CO_3}, where P represents $Gly_2HisGly$ or Gly_2Ha. $E^{0\prime}$ is a formal reduction potential based on concentrations rather than activities and $\Delta E = E^{\circ\prime} - E_{CO_3}$.

$$Ni^{III}(H_{-2}P)(H_2O)_2 + CO_3^{2-} \overset{K_{CO_3}}{\rightleftharpoons} Ni^{III}(H_{-2}P)(H_2O)(CO_3)^{2-} + H_2O \quad (4)$$

$$Ni^{III}(H_{-2}P)(H_2O)_2 \overset{K_{a1}}{\rightleftharpoons} Ni^{III}(H_{-2}P)(H_2O)(OH)^{-} + H^{+} \quad (5)$$

$$Ni^{III}(H_{-2}P)(H_2O)_2 + e^{-} \rightleftarrows Ni^{II}(H_{-2}P)^{-} + 2H_2O \quad (6)$$

$$\exp\left[\Delta E\left(\frac{nF}{RT}\right)\right] = \left(1 + \frac{K_{a1}}{[H^+]}\right) + K_{CO_3}[CO_3^{2-}] \quad (7)$$

Figure 3 shows a plot of exp[$\Delta E(nF/RT)$] vs [CO_3^{2-}] for $Ni(III)Gly_2Ha$ where the slope of the line corresponds to the equilibrium constant, K_{CO_3}. Equilibrium constants calculated for the carbonate constants of $Ni(III)Gly_2Ha$ and $Ni(III)Gly_2HisGly$ are 85(10) M^{-1} and 52(4) M^{-1}, respectively. The intercept of the line in Figure 3 is $(1+K_{a1}/[H^+])$, and pK_{a1} values for the deprotonation constants are 9.3(2) for $Ni(III)Gly_2Ha$ and 9.3(1) for $Ni(III)Gly_2HisGly$. At this p[H$^+$], the spectrum of the complex is essentially the same as it is in acidic or neutral p[H$^+$]. These calculated pK_{a1} values have high uncertainties; however, the electrode potential measurements were also carried out as a function of p[H$^+$] which gave more precise pK_{a1} values.

Effect of Imidazole and Axial Water Deprotonation on the Electrode Potentials. Electrode potentials for the $Ni^{III/II}(H_{-2}Gly_2Ha)^{+/0}$ and $Ni^{III/II}(H_{-2}Gly_2HisGly)^{0/-}$ couples were measured as a function of p[H$^+$] with 5 mM $[CO_3]_{tot}$ present. Equation 6 corresponds to the reduction of Ni(III) to Ni(II), while eqs 5 and 8 represent consecutive deprotonations of the

$$Ni^{III}(H_{-2}P)(H_2O)(OH)^{-} \overset{K_{a2}}{\rightleftharpoons} Ni^{III}(H_{-3}P)(H_2O)(OH)^{2-} + H^{+} \quad (8)$$

complex. Equations 5, 6, and 8 are used to derive eq 9, where the imidazole deprotonation constant, K_{a2} (eq 8), was determined from the initial absorbance data. A value of $10^{-10.50(5)}$ M was determined for $Ni(III)Gly_2Ha$ (Figure 5). K_{a1} and $E^{\circ\prime}$ values are evaluated from the nonlinear least-squares fit of the data to eq 9 (Figure 4). The Ni(III) complex coordinated by CO_3^{2-} does not appear to lose a proton from the remaining axial water, and this is taken into account in eq 9. The formal reduction potential of $Ni^{III/II}(H_{-2}Gly_2Ha)^{+/0}$, evaluated from the fit of the data, is 0.928(4) V (vs NHE),

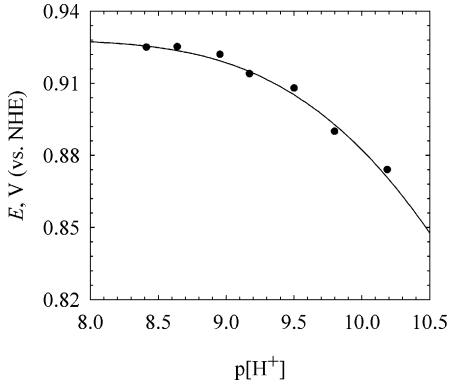

Figure 4. Plot of E (vs NHE) vs p[H$^+$] for $Ni^{III/II}(Gly_2Ha)^{+/0}$ couple, 25.0 °C, μ = 1.0 M, p[H$^+$] is controlled by using 5 mM $[CO_3]_T$. $[Ni(II)Gly_2Ha] = 1.0 \times 10^{-3}$ M. E° = 0.928(4) V, pK_a = 9.44(6).

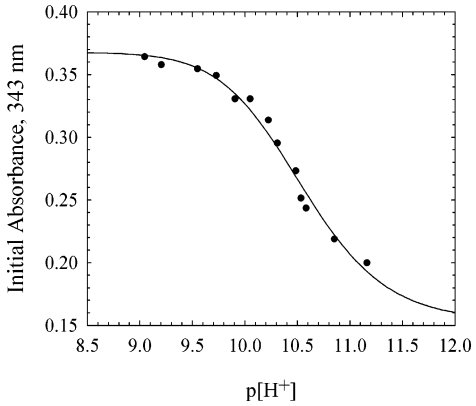

Figure 5. Initial absorbance of $Ni(III)Gly_2Ha$ as function of p[H$^+$]. $[Ni(III)Gly_2Ha]_{initial} = 9.5 \times 10^{-5}$ M, path length = 0.962 cm, 25.0 °C, μ = 1.0 M, is 50 mM $[CO_3]_{tot}$ except the last two data points where the buffer is 50 mM $[PO_4]_{tot}$. The solid line is calculated based on eq 8 and a pK_{a2} of 10.50(7) is obtained.

and the deprotonation constant of the axially coordinated water molecule gives a pK_a value of 9.44(6).

$$E = E^{\circ\prime} - \frac{RT}{nF}\ln\left(\frac{K_{a1}[H^+] + K_{a1}K_{a2} + K_{CO_3}[CO_3^{2-}][H^+]^2 + [H^+]^2}{[H^+]^2}\right) \quad (9)$$

For $Ni(III)Gly_2HisGly$, the value of K_{a2} could not be determined due to the fast decay of the complex above p[H$^+$] 10. However, K_{a2} has little effect on the evaluation of K_{a1} ($10^{-9.37(2)}$ M) for the $Ni(III)Gly_2HisGly$ complex. The formal reduction potential of $Ni^{III/II}(H_{-2}Gly_2HisGly)^{0/-}$ couple, evaluated from the fit of the data to eq 9, is 0.960(4) V (vs NHE).

In contrast, deprotonation of the axially coordinated water molecule was not observed below pH 11 with non-histamine/histidine-containing Ni(III) complexes.[24,25] Murray[24] estimated the pK_a value of the coordinated water molecule to be greater than 11 based on reduction potential measurements of the Ni(III)−peptide complexes in the pH range of 6.5 to 10.5. Similarly, Kirvan[25] found that the pK_a of a coordinated

(25) Kirvan, G. E.; Margerum, D. W. *Inorg. Chem.* **1985**, *24*, 3245−3253.

water in Ni(III)Ala_3 complex to be 11.3. In the present work, the much lower pK_a value for the axially coordinated water may be due to the π back-bonding nature of the imidazole ring.

The Cu(III)−peptide complexes, which do not contain axial waters, exhibit a significant pK_a decrease when histamine or histidine groups are in the third residue.[26,27] UV−vis spectra show that this deprotonation occurs at the N-terminal amine. This pK_a decrease was attributed in part to the π back-bonding ability of the imidazole group. Although the Ni(III) complexes in the current study do not form stable amine-deprotonated species,[10] the π back-bonding appears to affect the pK_a values for axial water deprotonation.

Kinetics. Ni(III)−peptide complexes with histidine and histamine as the third residue are relatively stable in acidic solution with half-lives of more than 10 h. However, in basic solution Ni(III)−peptide complexes are unstable, and the loss of Ni(III) is complete within milliseconds to seconds. The kinetics of Ni(III)Gly_2HisGly and Ni(III)Gly_2Ha decomposition were studied over the p[H^+] range of 3.5 to 10. At p[H^+] less than 7.0, the loss of the complex is first-order in Ni(III), while at p[H^+] above 8.5 the reaction is predominantly second-order in Ni(III). From p[H^+] 7.0 to 8.5, the loss of the Ni(III)−peptide complex is mixed-order, with first- and second-order dependencies in Ni(III) (eq 10). Between p[H^+] 7.0 and 8.5, first- and second-order rate constants are resolved from an integrated rate expression (eq 11).

$$\frac{-\mathrm{d}[\mathrm{Ni^{III}(peptide)}]_{tot}}{\mathrm{d}t} = k_1[\mathrm{Ni^{III}(peptide)}]_{tot} + k_2[\mathrm{Ni^{III}(peptide)}]^2_{tot} \quad (10)$$

$$A_t = \frac{A_o k_1 \exp(-k_1 t)}{k_1 + k_2(A_o - A_o \exp(-k_1 t))} + A_\infty \quad (11)$$

First-Order Path. A mechanism is proposed in eqs 12−17 to describe the loss of Ni(III) where the decay of the trivalent-metal complex is first-order in Ni(III). The observed first-order rate constants increase with both a first- and second-order dependence in [OH^-] (Figure 6). This suggests that both the diaquo and the axially deprotonated Ni(III) complexes are reactive species. The observed first-order rate also has a dependence on the basic form of acetate and phosphate buffers. The proposed mechanism includes the axial water deprotonation (eq 12), hydroxide path (eqs 13 and 14), the buffer path (eq 15), and the self-decomposition path (eq 16). Previous work[10,28] has shown that the reactivity of the $Ni^{III}(H_{-2}Gly_2Ha)^+$ and $Ni^{III}(H_{-2}Gly_2HisGly)$ complexes differ because they react via two- and four-electron oxidations, respectively. The parent peptide recoveries differ, and this stoichiometry is accounted for in eq 17, where n is 2 for Ni(III)Gly_2Ha (with ∼50% recovery)[28] and 4 for Ni(III)Gly_2HisGly (with 75% recovery).[10] The final product of $Ni^{III}(H_{-2}Gly_2HisGly)$ decomposition is $Ni^{II}(H_{-2}$oxamylglycylhistidylglycine$)^-$ (eq 17, Scheme 2).[10] The proposed intermediate in eqs 13−17 is shown in Scheme 2.

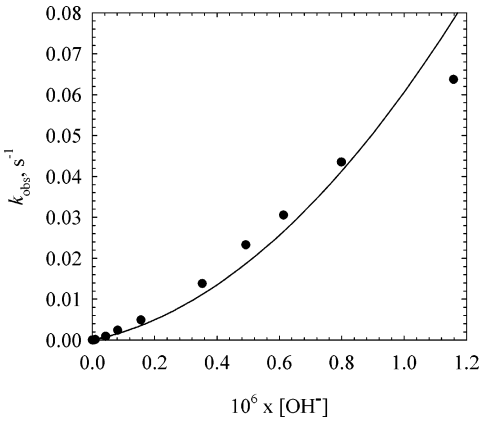

Figure 6. Dependence of the observed first-order rate constant on [OH^-] for $Ni^{III}(H_{-2}Gly_2HisGly)$. Conditions: 25.0 °C, μ = 1.0 M.

$$\mathrm{Ni^{III}(H_{-2}P)(H_2O)_2} \overset{K_{a1}}{\rightleftharpoons} \mathrm{Ni^{III}(H_{-2}P)(H_2O)(OH)^-} + \mathrm{H^+} \quad (12)$$

$$\mathrm{Ni^{III}(H_{-2}P)(H_2O)_2} + \mathrm{OH^-} \xrightarrow{k_1} \text{reactive intermediate} \quad (13)$$

$$\mathrm{Ni^{III}(H_{-2}P)(H_2O)(OH)^-} + \mathrm{OH^-} \xrightarrow{k_2} \text{reactive intermediate} \quad (14)$$

$$\mathrm{Ni^{III}(H_{-2}P)(H_2O)_2} + \mathrm{B^-} \xrightarrow{k_B} \text{reactive intermediate} \quad (15)$$

$$\mathrm{Ni^{III}(H_{-2}P)(H_2O)_2} \xrightarrow{k_d} \text{reactive intermediate} \quad (16)$$

$$\text{reactive intermediate} + n\mathrm{Ni^{III}(H_{-2}P)(H_2O)_2} \xrightarrow{\text{fast}} \mathrm{Ni^{II}(H_{-2}oxamylglycylhistidylglycine)^-} \quad (17)$$

The rate expression is given in eq 18, where $[Ni^{III}]_{tot} = [Ni^{III}(H_{-2}P)(H_2O)_2] + [Ni^{III}(H_{-2}P)(H_2O)(OH)^-]$. The values k_{obs} and k'_{obs} in eqs 18−21 are the observed first-order rate constants in the presence and absence of buffer, respectively, and $[HB]_{tot} = [HB] + [B^-]$. The general base dependence (eq 19) is shown in greater detail in eqs 20 and 21, where the OH^- and buffer paths are separated. The values of k_B are calculated from the acetate and phosphate buffer dependence studies and are used to correct k_{obs} in order to evaluate

(26) McDonald, M. R.; Scheper, W. M.; Lee, H. D.; Margerum, D. W. *Inorg. Chem.* **1995**, *34*, 229−237.
(27) McDonald, M. R.; Fredericks, F. C.; Margerum, D. W. *Inorg. Chem.* **1997**, *36*, 3119−3124.
(28) Green, B. J.; Tesfai, T. M.; Margerum, D. W. *J. Chem. Soc., Dalton Trans.* Submitted for publication.

Scheme 2. First-Order Pathway (k_2) of $Ni^{III}(H_{-2}Gly_2HisGly)$ Self-Decomposition[a]

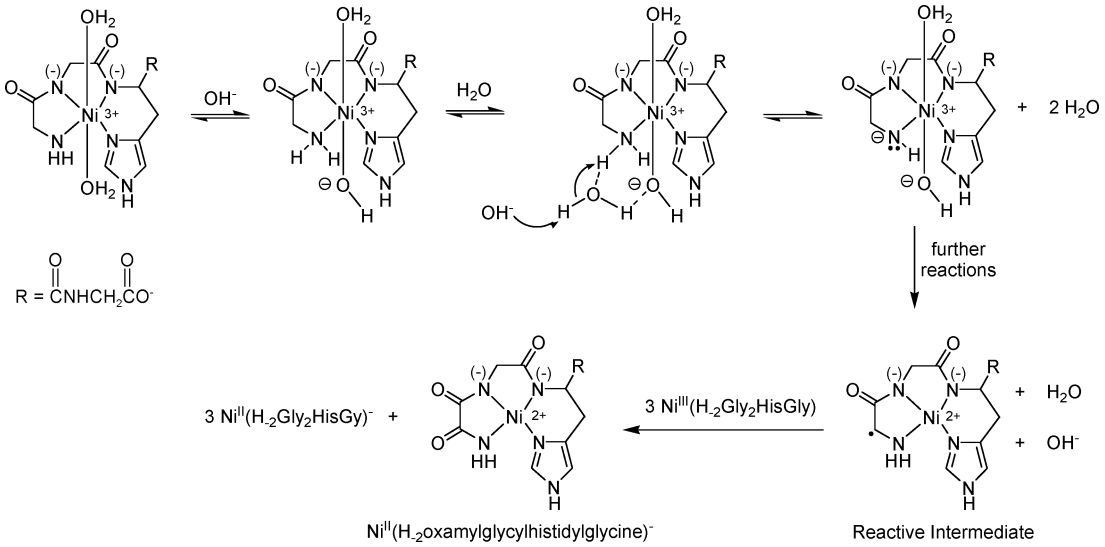

[a] The $Ni^{II}(H_{-2}$oxamylglycylhistidylglycine$)^-$ product was identified in previous work.[10]

Table 2. Summary of Rate and Equilibrium Constants for the Ni(III)Gly_2HisGly and Ni(III)Gly_2Ha Complexes[a]

	Ni(III)Gly_2HisGly	Ni(III)Gly_2Ha
k_d, s^{-1}	$3.5(9) \times 10^{-6}$	$2.1(9) \times 10^{-6}$
k_1, $M^{-1}\,s^{-1}$	$3.9(8) \times 10^{3}$	$7(3) \times 10^{2}$
k_2, $M^{-1}\,s^{-1}$	$7(2) \times 10^{5}$	$4.2(8) \times 10^{5}$
pK_{a1} [b]	9.37(8)	9.44(8)
pK_{a2} [c]		10.50(5)
K_{CO3}, M^{-1}	52(4)	85(10)
kK', $M^{-1}\,s^{-1}$	79(1)[d]	16(2)

[a] Conditions: 25.0 °C, $\mu = 1.0$ M ($NaClO_4$). [b] The deprotonation of the axially coordinated water molecule and calculated from electrochemical measurements. [c] The deprotonation constant of the imidazole ring was calculated from absorption measurements. [d] An estimated pK_{a2} value of 10.50 was used to calculate kK'.

k'_{obs} for the $[OH^-]$ dependence. The rate constants evaluated from the fit are summarized in Table 2.

$$\frac{-d[Ni^{III}]_{tot}}{dt} = k_{obs}[Ni^{III}]_{tot} \tag{18}$$

$$k_{obs} = \frac{n\left(k_d + k_1[OH^-] + \frac{k_2K_{a1}}{K_w}[OH^-]^2 + k_B[B^-]\right)K_w}{K_w + K_{a1}[OH^-]} \tag{19}$$

$$k_{obs} = k'_{obs} + n\left(\frac{K_wk_B}{K_w + K_{a1}[OH^-]}\right)\left(\frac{K_a^{HB}[HB]_{tot}}{K_a^{HB} + [H^+]}\right) \tag{20}$$

$$k'_{obs} = \frac{n\left(k_d + k_1[OH^-] + \frac{k_2K_{a1}}{K_w}[OH^-]^2\right)K_w}{K_w + K_{a1}[OH^-]} \tag{21}$$

Assistance of a general base in the loss of Ni(III) complex shows that proton abstraction is the rate-determining step. General-base assisted rate constants follow the Brønsted-Pedersen relationship of eq 22,[29] where p is the number of equivalent protons in acid HB, q is the number of sites that can accept a proton in a conjugate base B^-, G_B is a constant, and β can be considered

Table 3. Summary of Constants for the Brønsted Relationship in the Decay of $Ni^{III}(H_{-2}P)(H_2O)_2$[a]

B^-	p[b]	q[c]	pK_a^{HB}	Ni(III)Gly_2HisGly k_B, $M^{-1}\,s^{-1}$	Ni(III)Gly_2Ha k_B, $M^{-1}\,s^{-1}$
H_2O	3	2	−1.74[d]	$6(2) \times 10^{-8}$ [e]	$4(2) \times 10^{-8}$ [e]
$H_2PO_4^{2-}$	3	2	1.70	$4.3(1) \times 10^{-5}$	$1.95(2) \times 10^{-5}$
CH_3COO^-	1	2	4.55	$1.72(3) \times 10^{-3}$	$7.69(4) \times 10^{-4}$
OH^-	2	3	15.39[f]	$3.9(8) \times 10^{3}$	$7(3) \times 10^{2}$

[a] Conditions: 25.0 °C, $\mu = 1.0$ M ($NaClO_4$). [b] p is the number of equivalent proton sites on HB. [c] q is the number of equivalent basic sites on B^-. [d] $-\log(55.5)$. [e] $k_B = k_d/55.5$. [f] $pK_a^{HB} = pK_w + \log(55.5)$.

$$\log\left(\frac{k_B}{q}\right) = \log G_B + \beta\log\left(\frac{p}{qK_a^{HB}}\right) \tag{22}$$

to be the degree of proton transfer in the transition state that ranges from 0 to 1. Table 3 summarizes the values of p, q, k_B, and K_a^{HB} values of water, phosphate, acetate, and hydroxide. A Brønsted-Pedersen plot is shown in Figure 7 with a slope (β) of 0.62(4) for Ni(III)Gly_2HisGly and 0.59(3) for the Ni(III)Gly_2Ha complex. Brønsted values of 0.61(5) reflect a relatively large degree of proton transfer for k_B (eq 13) to give the reactive intermediate. These values reflect the decomposition of $Ni^{III}(H_{-2}P)(H_2O)_2$ and not $Ni^{III}(H_{-2}P)(H_2O)(OH)^-$. It should also be noted that this general-base assistance is evidence that the k_1 and k_B paths in eqs 13 and 15 represent proton abstraction directly from the ligand by OH^- and B^- rather than internal conversion by an axial hydroxide group.

We propose that the reaction at the first glycyl residue occurs by proton abstraction from the terminal amine, which initiates the rate-determining oxidation step. The Ni(III)-deprotonated amine complex reacts further to give Ni(II) and a radical at the α-carbon (Scheme 2). This radical can reduce

(29) Bell, R. P. *The Proton in Chemistry*, 2nd ed.; Cornell University: Ithaca, NY, 1973; p 198.

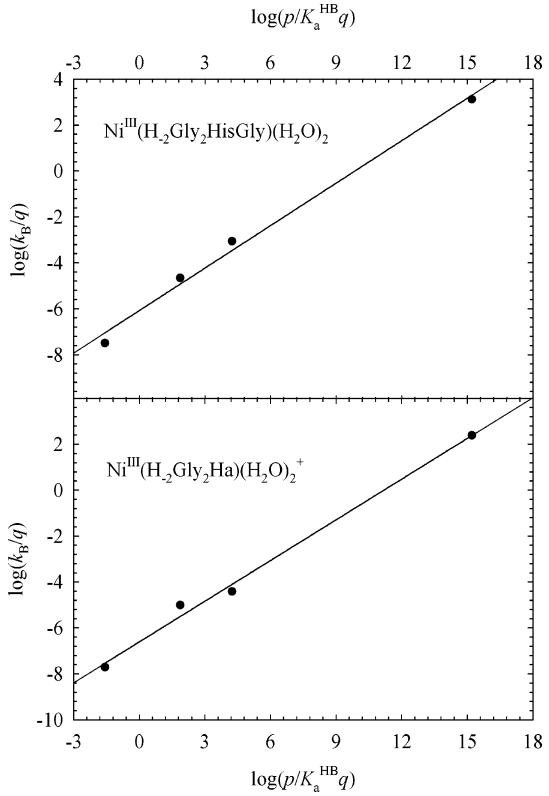

Figure 7. Brønsted plots for the reactions of $Ni^{III}(H_{-2}Gly_2HisGly)(H_2O)_2$ and $Ni^{III}(H_{-2}Gly_2Ha)(H_2O)_2^+$ with bases (B^-), where k_B is the second-order rate constant and K_a^{HB} is the ionization constant of HB. Slope (β) = 0.62(4) for $Ni^{III}(H_{-2}Gly_2HisGly)(H_2O)_2$ and 0.59(3) for $Ni^{III}(H_{-2}Gly_2Ha)(H_2O)_2^+$.

a second Ni(III)−peptide complex to Ni(II). The carbocation intermediate formed in the previous step hydroxylates rapidly in solution and reacts further to form Ni^{II}(H_{-2}oxamylglycylhistidylglycine).[10]

In eqs 13 and 14, the rate constant k_2 is approximately 2 orders of magnitude larger than k_1 for both complexes. The deprotonation of the coordinated water molecule to give a hydroxide group at the axial site gives a more reactive species with a base than when water is coordinated to the Ni(III)−peptide complex. We propose that this increased rate is due to the axially coordinated hydroxide group assisting proton abstraction from the N-terminal amine via a water bridge (Scheme 2). The formation of a hydrogen bond between oxygen from water and amine proton could promote the proton abstraction that leads to the rate-determining step. The rate constants evaluated from the first-order path are given in Table 2.

Second-Order Path. Previous studies of Ni(III)−peptide complexes without histamine or histidine groups have shown a first-order decay of Ni(III) in basic solution.[25] However, the present work shows that the Ni(III) complexes of histamine and histidine exhibit second-order decay. One difference is that the histamine/histidine-containing complexes deprotonate with pK_a values of 9.3−9.5, while the non-histidine/histamine complexes have pK_a values of greater than 11.[24,25]

Oxo-bridged dinuclear Ni(III) complexes have been reported.[10,30] In the present study, we propose that the formation of an oxo bridge between two Ni(III) complexes leads to a Ni(III)−peptide dimer intermediate (Scheme 3). This reactive intermediate could be formed when an axially deprotonated hydroxyl group displaces an axial water from another Ni(III) complex to form the oxo-bridged dimer.

We do not see general-base assistance by HPO_4^{2-} or CO_3^{2-} in the decay of the dimer, perhaps because of the dominant OH^- path at higher pH. However, carbonate suppresses the rate of decay because of its ability to axially coordinate to the complex and stabilize Ni(III) (Scheme 1). An overall reaction mechanism is proposed for the second-order path in eqs 12 and 23−26. K_{a1} represents deprotonation of the axially coordinated water molecule, and K_{a2} represents the deprotonation of the imidazole nitrogen. The values of K_{a1} and K_{a2} used for Ni(III)Gly_2Ha are $10^{-9.44}$ and $10^{-10.50}$ M, respectively. K_B is an equilibrium constant for the exchange of buffer with the axially coordinated water molecule.

$$Ni^{III}(H_{-2}P)(H_2O)_2 \overset{K_{a1}}{\rightleftharpoons} Ni^{III}(H_{-2}P)(H_2O)(OH)^- + H^+ \quad (12)$$

$$Ni^{III}(H_{-2}P)(H_2O)(OH)^- \overset{K_{a2}}{\rightleftharpoons} Ni^{III}(H_{-3}P)(H_2O)(OH)^{2-} + H^+ \quad (23)$$

$$Ni^{III}(H_{-2}P)(H_2O)_2 + CO_3^{2-} \overset{K_B}{\rightleftharpoons} Ni^{III}(H_{-2}P)(H_2O)(CO_3)^{2-} + H_2O \quad (24)$$

$$Ni^{III}(H_{-2}P)(H_2O)_2 + Ni^{III}(H_{-2}P)(H_2O)(OH)^- \overset{K'}{\rightleftharpoons} [Ni^{III}(H_{-2}P)(H_2O)]_2(O)^{2-} + H^+ \quad (25)$$

$$[Ni^{III}(H_{-2}P)(H_2O)]_2(O)^{2-} + OH^- \overset{k}{\rightarrow} \text{cross-linked peptide} \quad (26)$$

$$\frac{-d[Ni^{III}]_{total}}{dt} = k_{2,obs}[Ni^{III}]_{total}^2 \quad (27)$$

The rate expression is given in eq 27, where $[Ni^{III}]_{tot} = [Ni^{III}(H_{-2}P)(H_2O)_2] + [Ni^{III}(H_{-2}P)(H_2O)(OH)^-] + [Ni^{III}(H_{-3}P)(H_2O)(OH)^{2-}] + [Ni^{III}(H_{-2}P)(H_2O)(CO_3)^{2-}]$. An oxo-bridged Ni(III) species is formed as a result of the preequilibrium (eq 25) between two axially-deprotonated Ni(III) complexes. This dimer is a very reactive intermediate. Equation 28 gives the observed second-order rate constant as a function of buffer and hydroxide concentration. The effect of CO_3^{2-} was corrected by performing a carbonate dependence study at p[H^+] 9.38. The observed second-order rate constants were independent of phosphate, and, therefore, no correction was

(30) Bag, B.; Mondal, N.; Rosair, G.; Mitra, S. *Chem. Commun.* **2000**, 1729−1730.

Scheme 3. Second-Order Pathway of Ni(III)−Peptide Self-Decomposition[a]

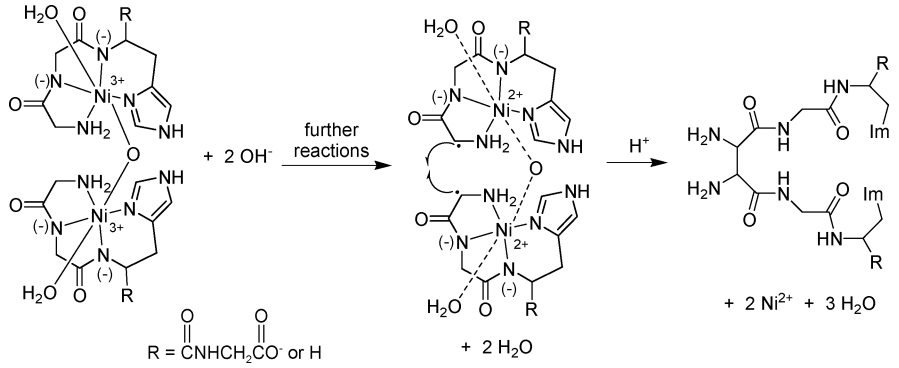

[a] The cross-linked peptide product was identified previously.[10]

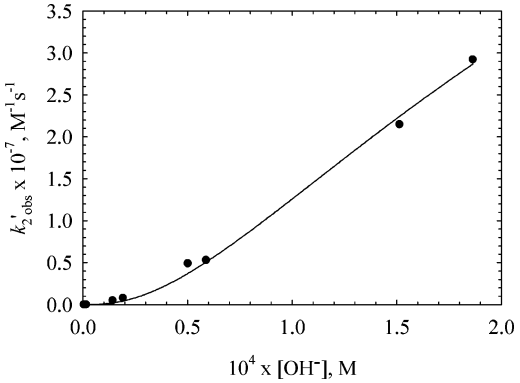

Figure 8. Dependence of the second-order rate constant on [OH^-] for $Ni^{III}(H_{-2}Gly_2HisGly)$. Conditions: 25.0 °C, $[Ni^{III}(H_{-2}Gly_2Ha)^+]_{tot} = 0.05$ mM, $\mu = 1.0$ M. The solid line is a fit of eq 29 using an estimated K_{a2} value of $10^{-10.50}$. A kK' value of 79(1) M^{-1} s^{-1} was obtained from the fit.

performed. After the effect of buffer was corrected, the data were fit to eq 29.

$$k_{2,\mathrm{obs}} = \frac{2(kK'K_{a1}[OH^-]^3)}{K_w^2\left(1 + \frac{K_{a1}}{K_w}[OH^-] + \frac{K_{a1}K_{a2}}{K_w^2}[OH^-]^2 + K_B[B^-]\right)^2} \quad (28)$$

$$k_2'_{\mathrm{obs}} = \frac{2(kK'K_{a1}[OH^-]^3)}{K_w^2\left(1 + \frac{K_{a1}}{K_w}[OH^-] + \frac{K_{a1}K_{a2}}{K_w^2}[OH^-]^2\right)^2} \quad (29)$$

In eq 29, the only unknown terms are k and K'. These values cannot be determined independently. However, the product of k and K' was determined from a nonlinear least-squares fit of eq 29. The kK' value calculated for Ni(III)-Gly_2HisGly is 79(1) M^{-1} s^{-1}. Since the K_{a2} value for Ni(III)Gly_2HisGly could not be measured, the value for Ni(III)Gly_2Ha ($10^{-10.50}$) was used to fit eq 29 (Figure 8). A $kK' = 16(2)$ M^{-1} s^{-1} was obtained for Ni(III)Gly_2Ha. The fact that the reactions remain second order even at pH > 8.5 indicates that the value of K' is relatively small and that k is large. The concentration of the oxo-bridged dimer at any given time is very small.

Scheme 3 shows the self-decomposition of the oxo-bridged Ni(III)−peptide dimer to give a cross-linked peptide. Similar to what is proposed in the first-order path (Scheme 2), base-assisted deprotonation of the N-terminal amine initiates a rate-determining step. This is followed by fast reactions that include reduction of Ni(III) to Ni(II) and the concurrent formation of an α-carbon radical, Ni^{2+}−O bond breakage, and C−C bond formation. The final product is the cross-linked peptide.[10]

Conclusions

The rates of decomposition of Ni(III)−peptide complexes that contain histidine or histamine as the third residue have a complex pH and buffer dependence as well as a variable reaction order in Ni(III) concentration. Mechanisms are proposed to explain this behavior. Ni(III)Gly_2HisGly and Ni(III)Gly_2Ha exhibit similar kinetics, although Ni(III)Gly_2Ha consistently decays more slowly. Both Ni(III)−peptides undergo axial water deprotonation with $pK_{a1} = 9.4$ and a second deprotonation at the imidazole nitrogen at higher pH where $pK_{a2} = 10.5$ for Ni(III)Gly_2Ha. (Imidazole deprotonation of the Ni(II) complexes is more difficult, thus the pK_{a2} value for Ni(II)Gly_2Ha is 11.54.) The second-order Ni(III) dependence is attributed to the formation of an oxo-bridged Ni(III)−peptide dimer that yields a cross-linked peptide as a product.

Acknowledgment. This work was supported by National Science Foundation Grants CHE-9818214 and CHE-0139876. The authors also wish to thank Dr. H. D. Lee for the Gly_2-Ha synthesis and purification.

Supporting Information Available: Tables and figures with supplemental data. This material is available free of charge via the Internet at http://pub.acs.org.

IC049338A